

# Investigations and Characterization of Extrusion Based Additively Manufactured PEEK for Biomedical Applications

Jasvir Singh, Vishal Francis\*

School of Mechanical Engineering, Lovely professional University, Punjab, India. \*Corresponding Author's Email: vishal.24813@lpu.co.in

## Abstract

Fabrication of complex geometrical features is the major requirement for various biomedical applications. Due to specific anatomical features of patients, customization is to be provided in short period. The desire for improved biomedical implants is increasing interest in innovative techniques to improve implant functionality, customization, and performance. Additive manufacturing (AM) has shown promise for creating complex features in a shorter amount of time. Hence, there is a requirement to explore and analyse the additive manufacturing of biomaterials for various applications. Polyetheretherketone (PEEK) possesses good mechanical and thermal properties compared to other biopolymers. PEEK is bioactive biomaterial which can be used in AM. This paper explores mechanical and thermal behaviour of components fabricated via AM process. Moreover, the study examines the mesostructure of the additive manufactured PEEK and observes surface roughness. Based on the findings, the study suggests that additive manufacturing of PEEK material can be a viable option for various biomedical applications. These findings indicate that PEEK produced via additive manufacturing not only improves design freedom but also functionality, giving a possible road ahead in the development of customized, high-performance biomedical solutions. Integrating PEEK with other biocompatible materials may result in specific mechanical properties, making implants more suitable for replicating complex human tissues.

**Keywords:** Additive Manufacturing, Biomedical Application, PEEK, 3D Printing.

## Introduction

The technology of AM provides the freedom to fabricate highly intricate components as per the virtual design (1). This technology has been available for commercial and industrial use since it greatly improves the fabrication of components with precise geometries directly from CAD designs (2). The parts can be fabricated without the need of any tooling thereby reducing the cost involved (3). Furthermore, it is apparent that the additive technology's future scope and capabilities will extend far beyond 3D prototyping (4). During the early stages of development for 3D printing techniques, the primary motivation was the swift production of physical components without relying on conventional tooling methods (5). AM technology has the potential to achieve the objective of shorter lead times for production and the creation of products with highly intricate geometries (6). The Medical Additive Manufacturing/3D printing (AM3DP) 2020 Annual Report was published by SME, a professional association in the United States. This report offers a comprehensive summary

utilization of AM in the medical field, with a particular emphasis on the role of technical advancements in improving the cost-effectiveness of patient treatment (7). Based on a field study, 3D printed products, including both medical implants and devices, constitute 11% of the total revenue generated by the medical industry. The current necessity for customised medical solutions could explain this increased interest. Various imaging technologies utilized in the medical field can be employed to produce .STL files for 3D printing. This capability enables the creation of customized products for anatomical structures with complex medical requirements (8). Additive manufacturing has emerged to be a viable option to promote and explore health care sector, and has shown tremendous potential in tissue engineering, organs growth, anatomical models, construction of tailor - made implants and prosthetics, development in the pharmaceutical area, particularly in medication dosage varieties, discovery and delivery, and other biomedical uses of additive manufacturing are among the most

This is an Open Access article distributed under the terms of the Creative Commons Attribution CC BY license (<http://creativecommons.org/licenses/by/4.0/>), which permits unrestricted reuse, distribution, and reproduction in any medium, provided the original work is properly cited.

(Received 23<sup>rd</sup> September 2024; Accepted 22<sup>nd</sup> January 2025; Published 31<sup>st</sup> January 2025)

commonly used (9). Additive manufacturing has gained widespread acceptance in the medical field due to a multitude of benefits it offers, such as customized medical product design, biocompatibility, cost-effectiveness, improved productivity, enhanced accessibility, rapid turnaround times, simplified assembly, and democratization of the manufacturing process (10-14). Today many researchers have been constantly working on the exploration of an economical commercialization of the technology by focusing on the in house fabrication of FDM filaments using different polymer and polymer based biocompatible composite (15-20). However, in the medical field, where great level of precision and tailored products is required in small quantities, this limitation is seen as a

benefit. Additive manufacturing is a preferred option for clinical and biological applications due to the varying medical requirements and customized therapies for individual patients, making it an ideal solution to meet the diverse needs of patients (21-26). The layer-by-layer manufacturing technique provides the ability to break down the complex shapes into 2D layers which are build one layer at a time. The CT imaging details can be analysed and used to extract the necessary area for CAD model construction. The model can be fabricated for various medical applications (figure 1). These models provide better solution for targeting critical problems associated with human customised implant under biomedical treatment (27-30).

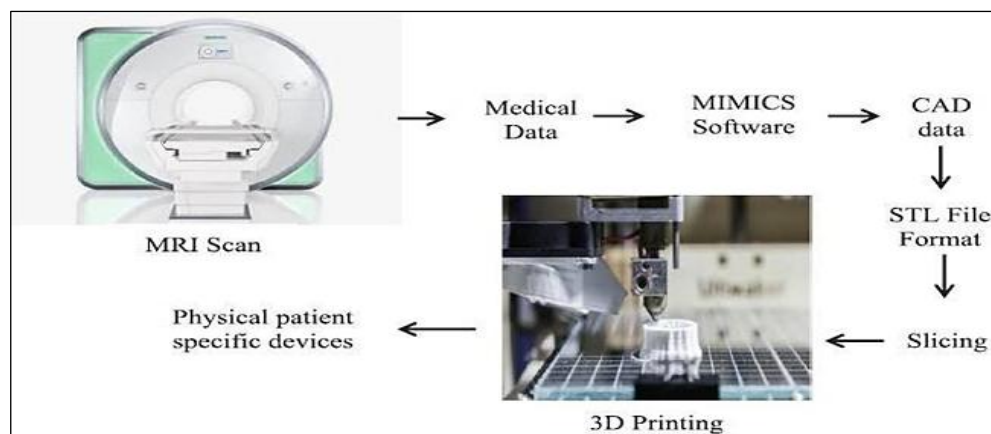


**Figure 1:** Patient Specific Fabrication of Additively Manufactured Part from Digital Data (31)

PEEK-based biomaterials are increasingly gaining popularity as a suitable option for bone and cartilage replacement, along with several other medical applications. PEEK has properties similar to the bone structure. This material can serve as an alternative to solve practical complications in the construction of customized complex biomedical implants through 3D printing (32). PEEK materials are gaining prominence in the medical field as they can be used to replace ceramic and titanium implants in various surgical procedures, making it crucial to investigate their efficacy in orthopaedic, spine, maxillofacial, and cranial surgeries. By utilizing 3D printing technology, complex design implants can be manufactured to meet the specific needs of each patient with an exact match. PEEK materials offer excellent wear and abrasion resistance, as well as a lower coefficient of friction (33). A prevalent

and promising form of AM is fused deposition modelling (FDM), which is utilized extensively for a variety of applications (34). The technology now allows for the creation of complicated topologies. With the ease of usage, there is no requirement for supervision, environmentally safe materials and low production cost (35). The material is heated up and pushed via an extrusion head during FDM printing, and then it is laid out onto a build platform (36, 37). The process starts by dividing the CAD model into layers using the .STL file format to provide a tooling route for the printer nozzle. The filament made of polymer material is fed through the nozzle to print the item (38). To preserve the feed material's capacity to flow through the nozzle, the temperature of the extruder head is regulated (39). In Figure 2, a schematic representation of this machine is shown.

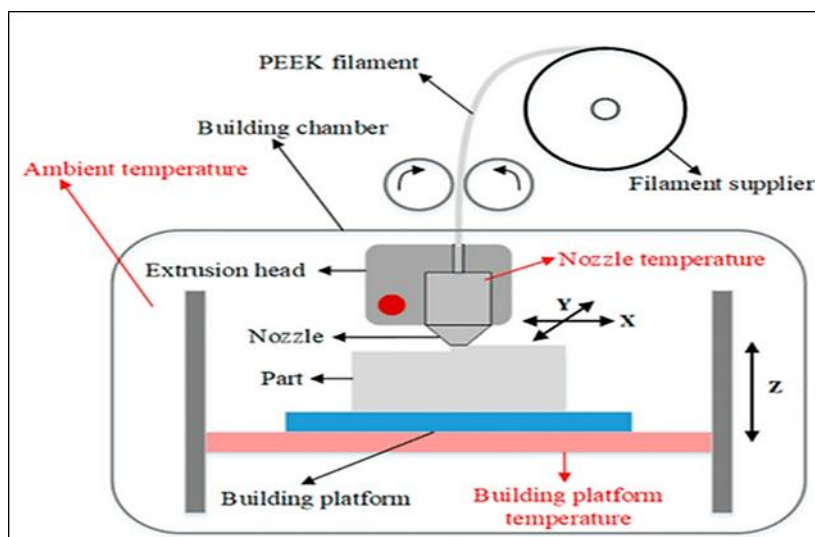


**Figure 2:** FDM Printer for PEEK (36)

Biomedical applications often use various biomaterials, such as PEEK and PAEK, in FDM technology. However, these materials are less accessible and more expensive, which increases the overall running costs of the FDM system (40). The paper explores the AM of PEEK material via FDM technique. In order to examine the properties of printed parts mechanical testings were carried out such as tensile, compression and impact test. The fabricated parts were characterized by SEM and XRD testing. Moreover, thermal properties were also investigated of the printed specimens. Surface roughness which also plays an important role in biomedical applications was observed. Most biocompatible materials exhibit low mechanical properties, with research primarily focusing on materials with lower strength compared to PEEK. There is a critical need to explore the effects of 3D printing on high-performance materials like PEEK. Comprehensive

studies are required to evaluate the material's performance under tensile, compressive, and impact loading conditions. Investigating the effects of high-temperature extrusion on the mechanical and thermal stability of PEEK is essential for its application in demanding biomedical environments. There is need to explore optimized machining parameters to improve printing accessibility of high-performance PEEK for a biomedical application.

## Methodology

Polyetheretherketone (PEEK) a thermoplastic biomaterial was used for the investigation. PEEK filament was supplied by Victrix (VICTREX AM™ 450 FIL) of diameter 1.75 mm and melting point of 343°C. The print head temperature was set as 450°C for all PEEK test specimens. The parameters used for fabrication of the specimens are listed in table 1.

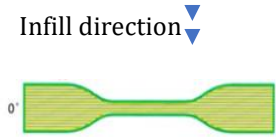
**Table 1:** Parameters Setting for Specimen Fabrication

Parameters	Control Setting of FDM Printer
Print Speed (mm/s)	40
Printing Temp (°C)	430
Bed temperature (°C)	130
Nozzle Temperature (°C)	410
Fill density %	100
Layer height (mm)	0.2
Extrusion width (mm)	0.35
Top layer Fill	4
Bottom layer Fill	4
Nozzle diameter (mm)	0.4

Table 2 illustrates the infill pattern chosen for each type of specimen. The tensile specimens were printed with an infill pattern along the tensile loading direction, while the compressive specimens had a pattern along the circumference,

and the impact specimens had a pattern perpendicular to the impact force. The dimensions of the specimens fabricated for investigations for mechanical testing's illustrated in table 3.

**Table 2:** Selection of Infill Patterns for Tensile, Compression and Impact test

Type of Test	Infill pattern	Analysis	Reference
Tensile Test (ASTM D638 type IV)		<p><b>Effect of Infill Orientation on Tensile Strength:</b></p> <p>a. When the infill lines are aligned with the tensile loading direction, the load is distributed more uniformly along the filament paths. This alignment minimizes stress concentrations and enhances load transfer efficiency.</p> <p>b. Misaligned or cross-hatched infill patterns often create stress risers at intersections, leading to premature failure. Parallel alignment reduces these weak points.</p> <p>c. The alignment ensures that the deposited material directly contributes to resisting tensile forces, optimizing the material's tensile strength potential. By designing the infill pattern in this manner, the tensile specimen exhibits greater strength and stiffness along the loading direction, resulting in improved mechanical performance.</p>	(41-43)
Compressive strength (ASTM D695)		<p><b>Effect of Circumferential Infill Orientation on Compressive Strength:</b></p> <p># The circumferential pattern enhances the ability of the specimen to distribute compressive forces evenly around the circumference, minimizing localized stress concentrations.</p> <p>#The circular alignment resists buckling by providing continuous support across the structure, particularly beneficial under axial compressive loads.</p> <p># The circumferential infill minimizes voids and discontinuities that could act as failure points, enhancing the overall compressive strength of the specimen.</p>	(44, 45)

Impact test (ASTMD256)

Load Application



**Effect of Perpendicular Infill Orientation on Impact Strength**

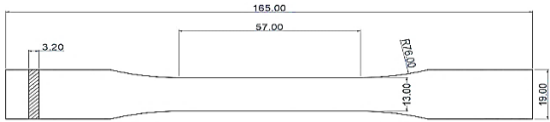
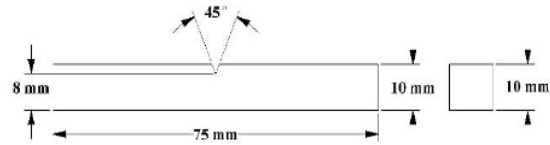
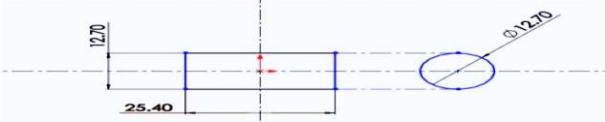
#The perpendicular arrangement of the infill lines enhances the specimen's ability to absorb and dissipate impact energy across multiple layers. This reduces the risk of crack propagation.

#The orientation creates more interfaces and barriers perpendicular to the force, which acts as obstacles to crack growth, improving fracture toughness under impact.

# When impact forces are applied, the perpendicular infill pattern redistributes the force across the structure, minimizing stress concentrations and delaying failure.

(46, 47)

**Table 3:** Dimension Details of Tensile, Impact and Compression as per ASTM

S.No.	Mechanical Test	Dimensions
1	Tensile	
2	Impact testing	
3	Compression	

## Results and Discussion

### Mechanical Characterization

Tensile tests were conducted based on ASTM D638 type IV to evaluate the tensile behaviour of polymers. The specimen dimension is 165x19x3.2 mm<sup>3</sup>. The peak load applied was 1988 N. As per the observation, the PEEK tensile specimen breaks at a tensile strength load of 51.52 MPa (Specimen 1), 46.182 MPa (Specimen 2) and 50.37 MPa (Specimen 3) with a percentage elongation of 496.7 %, 582.4 % and 561.2 % respectively. The high value of tensile strength is due to infill pattern which is along the direction of applied

tensile load. The state of polymeric chains is highly correlated to the tensile properties of polymers. The PEEK material is semi-crystalline in nature. The material has amorphous regions in along with crystalline regions. The crystalline region after 3D printing exhibits better alignment of chains. This provides better intermolecular force thereby offers strength of the part (figure 3). However, the chains in amorphous region do not align to that degree as crystalline region. This provides elongation to the specimens. The presence of a larger proportion of crystalline regions in specimens can potentially enhance the tensile properties and stiffness. Conversely, a

greater proportion of amorphous regions might lead to a significantly higher elongation at break

(48). Figure 4 shows the tensile and compression testing setup used for the study.

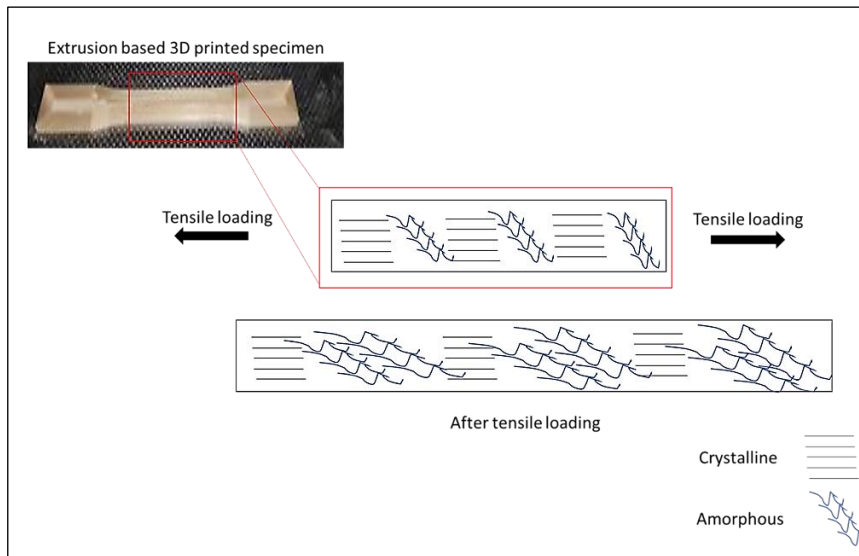


**Figure 3:** PEEK Specimen by FDM Printer having Amorphous and Crystalline Regions

The mechanical behaviour of pure virgin PEEK was observed to be significantly influenced by thermal processing conditions i.e., melt temperature, nozzle temperature, ambient temperature conditions, position and aggregation of macromolecular chains in crystalline and amorphous regions, molecular mobility of PEEK matrix during 3D printing. The compressive strength of PEEK sample was investigated to check the circumferential building bonding between the PEEK molecules during extrusion as illustrated in the figure 4. The standard specimens for compressive strength were found to be 272.42 MPa at a Load of 86 kN at a printing temperature of 430°C and nozzle temperature of 410°C. The obtained value of compression observed to be

significantly improved from the previous research. At a lower print temperature range of 360°C - 380°C, the PEEK material exhibit non uniform melt temperature produces incomplete melting region in the crystalline region causes lower interfacial bonding and poor fusion of the bottom interface result in a lower value of compressive strength. When the printing temperature is increased to a range between 420°C to 450°C, it can result in the supply of more heat energy which in turn produces a uniform melt and provides more time for crystallization. Additionally, if the temperature of the extruder nozzle much higher, it is more likely that polymer chains will be broken into shorter ones and undergo thermal degradation.

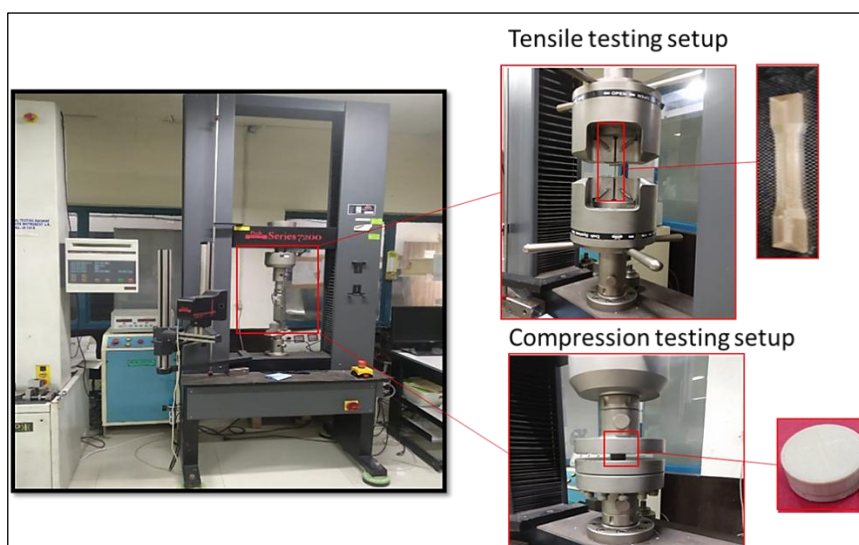


**Figure 4:** Tensile and Compression Testing of PEEK Specimens

The biomedical field frequently utilizes PEEK materials in implants such as hip stems, bone anchors, and cranial implants that are subjected to sudden impact. A significant effect on mechanical phenomena, such as changes in crystallinity, deformation, high strain rates and significant deformations related to impact, have been explored for PEEK. The failure occurs rapidly without any bending effect under high impact velocity, resulting in lower plastic work. The Izod Pendulum Impact Resistance of Plastics was determined for the impact samples fabricated as per ASTM D256 (64x12.7x3.2 mm<sup>3</sup>). Figure 5 illustrate the impact testing set-up used for the

study. Table 4 illustrates the experimental data of tensile, compression and impact testing. The thermal impact load causes deformation and delamination of standard impact PEEK specimen. Figure 6 illustrates visible deformation, such as warping and delamination, caused by the impact strain in the 3D printed PEEK specimens. PEEK is considered as a promising option for impact-resistant applications, including implants and passive security equipment like helmets. The impact strength is determined by measuring the energy absorbed by the specimen during the impact.

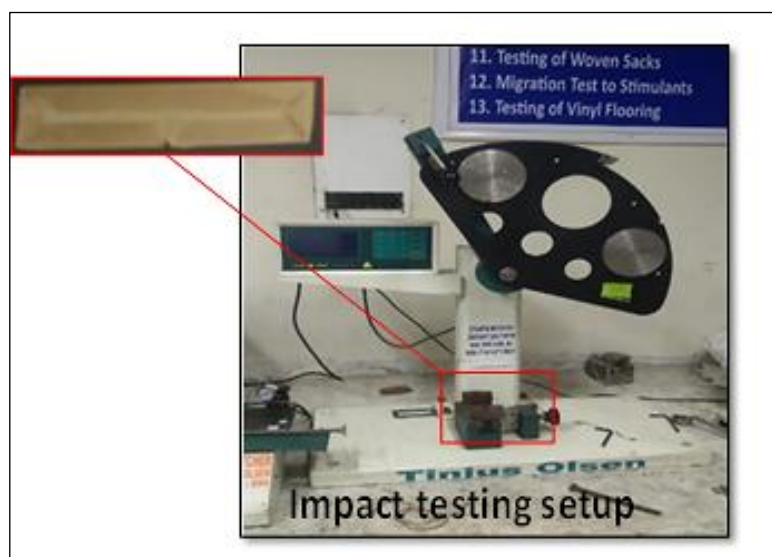


**Figure 5:** Impact Testing of PEEK Specimens

**Table 4:** Tensile and Compression Testing Results

Tensile Test	Unit	Sample 1	Sample 2	Sample 3	Standard Deviation
Tensile strength	MPa	51.52	46.18	50.37	2.8105
Young Modulus	MPa	1345.47	1435.75	1370.27	46.6425
Compressive Strength	MPa	272.42	268.6	279.91	4.737273
Impact Strength	KJ/m <sup>2</sup>	17.25	25.37	30.78	6.628591

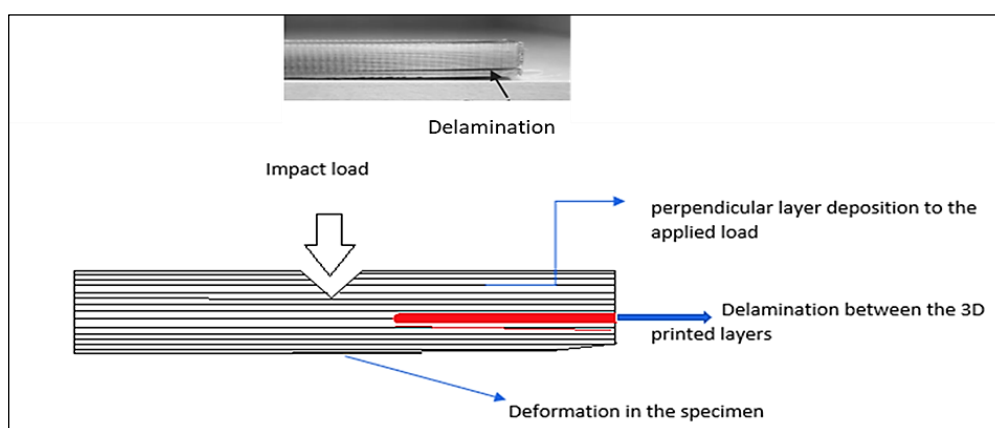


**Figure 6:** Delamination and Warping in the Specimens

Unmodified PEEK is less responsive to osteoconductive properties compared to metallic Titanium, which can affect osseointegration after implantation (49, 50). Surface topography alteration is a commonly used approach to enhance the biological performance of biomedical implants. Surface roughness can impact

biocompatibility by promoting cell proliferation, as a rough surface provides more binding sites for cells (51). The 3D printed specimens can have rough surface due to deposited layers these rough surfaces are at the boundary as well as at the top surface. The figure 7 shows surface produced by 3D printer (52).

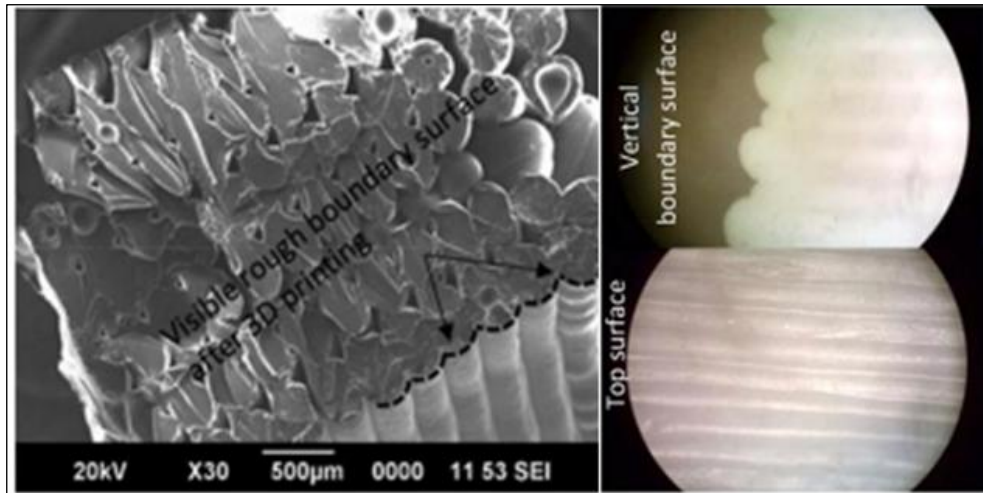


**Figure 7:** Surface Produced by 3D Printing Process (51)

Therefore, the obtained surface roughness values were investigated for the printed specimens. The surface morphology of printed specimens was

tested using an MITUTOYO SurfTest SJ-201P 2D contact stylus. Table 5 shows the measured surface roughness values.

**Table 5:** Surface Roughness of the Printed Specimens

Surface Roughness ( $\mu\text{m}$ )	*Ra	*Ry	*Rz	*Rq
Tensile Specimen1 (along Longitudinal)				
1	0.01	0.07	0.07	0.01
2	0.04	0.27	0.27	0.06
3	0.01	0.07	0.07	0.01
Average	0.02	0.13	0.14	0.02
Tensile Specimen1 (along Transverse)				
1	0.8	4.66	4.66	1.07
2	0.72	3.61	3.61	1.01
3	0.79	4.45	4.45	1.02
Average	0.77	4.24	4.24	1.03
Tensile Specimen 2 (along Longitudinal)				
1	0.01	0.06	0.06	0.01
2	0.01	0.04	0.04	0.01
3	0.01	0.07	0.07	0.01
Average	0.01	0.05	0.05	0.01
Tensile Specimen 2 (along Transverse)				
1	0.37	1.97	1.97	0.44
2	0.64	2.98	2.98	0.81
3	0.48	2.07	2.07	0.56
Average	0.50	2.34	2.34	0.603
Compression Specimen 1 (along Longitudinal)				
1	0.34	1.57	1.57	0.42
2	1.14	6.06	6.06	1.52

Average	0.74	3.81	3.81	0.97
Compression Specimen 1(along Transverse)				
1	0.48	2.85	2.85	0.67
2	0.42	2.03	2.03	0.55
Average	0.45	2.44	2.44	0.61
Compression Specimen 2 (along Longitudinal)				
1	2.65	2.19	2.19	1.6
2	1.39	2.59	3.59	0.84
Average	2.02	2.39	2.89	1.22
Compression Specimen 2 (along Transverse)				
1	0.76	3.38	3.38	0.93
2	0.51	2.47	2.47	0.65
Average	0.63	2.92	2.92	0.79
Impact Specimen 1 (along Longitudinal)				
1	0.54	2.62	2.62	0.69
2	0.28	1.33	1.33	0.35
Average	0.41	1.97	1.97	0.52
Impact Specimen 2 (along Transverse)				
1	1.08	4.75	4.75	1.29
2	0.7	3.71	3.71	0.91
Average	0.89	4.23	4.23	1.1

\*Ra = arithmetical mean roughness, Ry= maximum height, Rz= ten-point mean roughness, Rq =RMS Roughness

Surface roughness plays a critical role in determining the biological performance and functionality of biomaterials, particularly in applications like tissue engineering and implantable devices. After 3D printing, the surface characteristics of biomaterials such as PEEK, PLA, chitosan, PGA, and PLGA are inherently affected by the layer-by-layer deposition process, leading to notable roughness on both the boundary and top surfaces of the printed structures. The additive manufacturing process produces a surface with ridges and grooves due to the successive layering of material. This texture is more pronounced at the boundaries and the uppermost layers (53). The surface roughness varies based on the material's physical and thermal properties. PLA Known for its smooth deposition but may exhibit layer stratification due to rapid cooling (54). Chitosan being hydrophilic and softer, it may show uneven surface textures post-printing, especially under non-optimized conditions. PGA (Polyglycolic Acid) fast degradation rate can result in micro-roughness, which may enhance cellular interactions but necessitates controlled conditions to maintain integrity. The level of finishing obtained after 3D printing plays a crucial role in various biomedical

applications. According to technical observations, a surface roughness threshold of 0.2 micrometres, (Ra), has been considered clinically acceptable for biomedical implants (55). The rough surface of an implant can serve as a potential substrate for osseointegration, although it can also increase bacterial adherence due to the larger surface area (56). In the case of 3D-printed PEEK, the surface morphology appears to be conducive to sustaining cell proliferation necessary for proper functioning of biomedical implants.

### Statistical Analysis of Mechanical Properties

The mechanical test results for tensile strength, Young's modulus, compressive strength, and impact strength were analyzed to calculate the mean, standard deviation, and coefficient of variation (CV) has been shown in the Table 6. The results indicate consistent mechanical performance across the tested samples, with CV values ranging from 1.73% to 27.09%. The impact strength exhibited the highest variability (27.09%), while compressive strength showed the lowest (1.73%). This analysis highlights the reproducibility and reliability of the data across all configurations.

**Table 6:** Mechanical Test Results for the Mean, Standard Deviation, and Coefficient of Variation

Test	Unit	Mean	Standard Deviation	Coefficient of Variation (CV, %)
Tensile Strength	MPa	49.36	2.81	5.69
Young's Modulus	MPa	1383.83	46.64	3.37
Compressive Strength	MPa	273.64	4.74	1.73
Impact Strength	KJ/m <sup>2</sup>	24.47	6.63	27.09

The normality of the data was assessed using the Shapiro-Wilk test. The p-values for tensile strength ( $p = 0.394$ ), Young's modulus ( $p = 0.514$ ), compressive strength ( $p = 0.646$ ), and impact strength ( $p = 0.780$ ) indicate that the data for all

tests follow a normal distribution ( $p > 0.05$ ) as per Table 7. This confirms that parametric statistical methods, such as t-tests, are suitable for further analysis.

**Table 7:** Data Interpretation Values for the Mechanical Test Results

Test	W-Statistic	P-Value
Tensile Strength	0.9025	0.394
Young's Modulus	0.9366	0.514
Compressive Strength	0.9661	0.646
Impact Strength	0.9868	0.78

To evaluate the significance of the mechanical property results, one-sample t-tests were conducted against predefined benchmark values derived from industry standards and literature. The results in the table 8 and figure 8 showed no statistically significant differences between the

measured values and the benchmarks for tensile strength ( $p = 0.730$ ), Young's modulus ( $p = 0.609$ ), compressive strength ( $p = 0.723$ ), and impact strength ( $p = 0.905$ ). This indicates that the observed results align closely with expected performance metrics.

**Table 8:** T-sample Test Values to Evaluate the Significance of the Mechanical Property Results

Test	T-Statistic	P-Value
Tensile Strength	-0.396	0.73
Young's Modulus	-0.6	0.609
Compressive Strength	-0.408	0.723
Impact Strength	-0.136	0.905

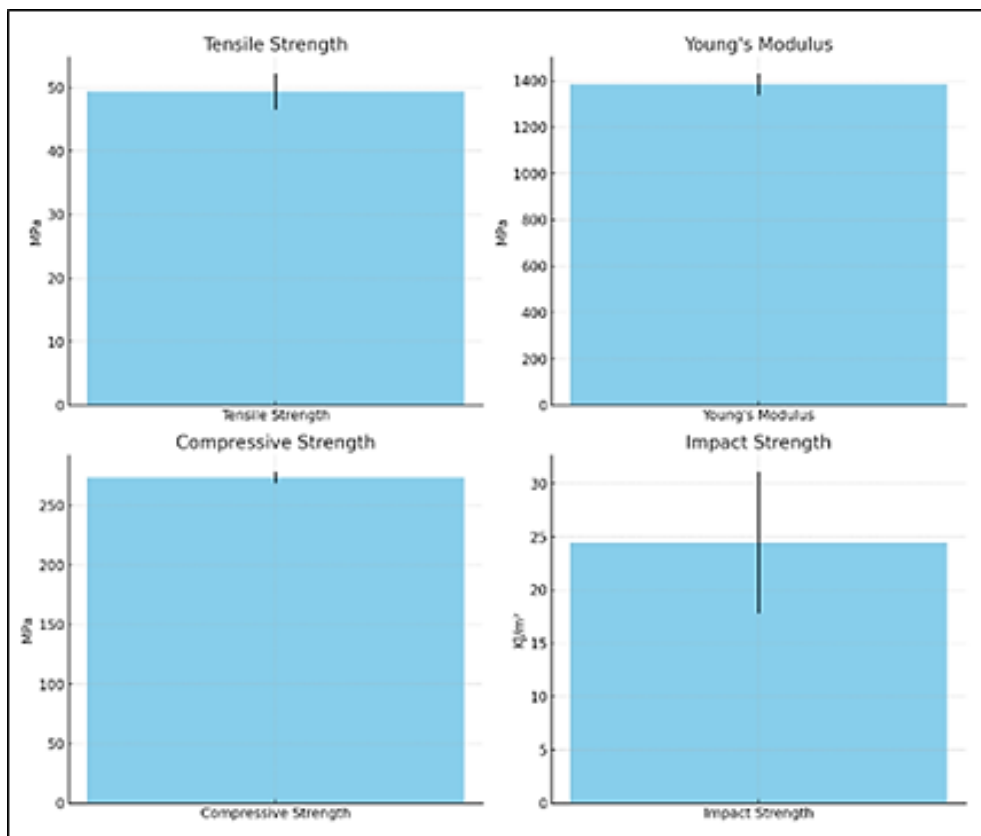


**Figure 8:** Illustrates Graphically the Achieved Tensile Strength, Young’s Modulus, Compressive Strength and Impact Strength

**Thermo Gravimetric Analysis**

The thermogravimetric test was conducted which involves heating the sample from 30.00°C to 900.00°C at a rate of 10.00°C/min with a sample weight of 5.489 mg, under a steady flow of nitrogen gas (20 mL/min. The TGA thermograms of virgin, PEEK is shown in figure 9. The PEEK shows thermal stability up to 558°C. The aromatic

rings in the polymer backbone contribute to PEEK's exceptional heat stability. Virgin PEEK began to degrade slowly around 560°C. The sample shows composition stage, that was a very fast step, for the range of 560 °C – 650 °C. After this temperature, again regaining constant behaviour is observed up to 900 °C.

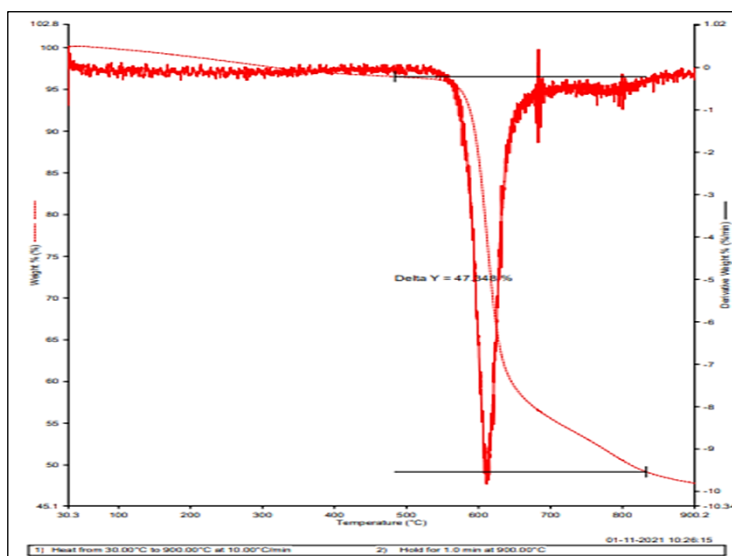


**Figure 9:** TGA Thermal Analysis of Virgin PEEK, Indicating Thermal Degradation Pattern of PEEK under Influence of Heat

The influence of heat addition over weight loss has been investigated as shown in figure 10. Up to 540°C very slow gradual rate of weight loss appears as shown in thermograph. Around 550°C, the remarkable weight loss occurred due to the loss of decomposition products of PEEK. In the case of virgin PEEK, the residual weight loss at 900°C was found to be around 47.348 %, which is due to the remaining ether and aromatic structures. The TGA thermographs indicate that most favourable temperature conditions for 3D print is before 550°C. The derivative weight (%/min) curve highlights the peak decomposition

temperature, which appears to occur near 600°C, corresponding to the maximum rate of weight loss as shown in figure 10. At 900°C, around 52% of the material remains, indicating the formation of thermally stable char or residue. This characteristic is common for high-performance polymers like PEEK, which exhibit high thermal stability and leave behind a significant carbonaceous residue. A comparison of mechanical and thermal properties is provided between the achieved results and other biocompatible polymer materials (table 9).

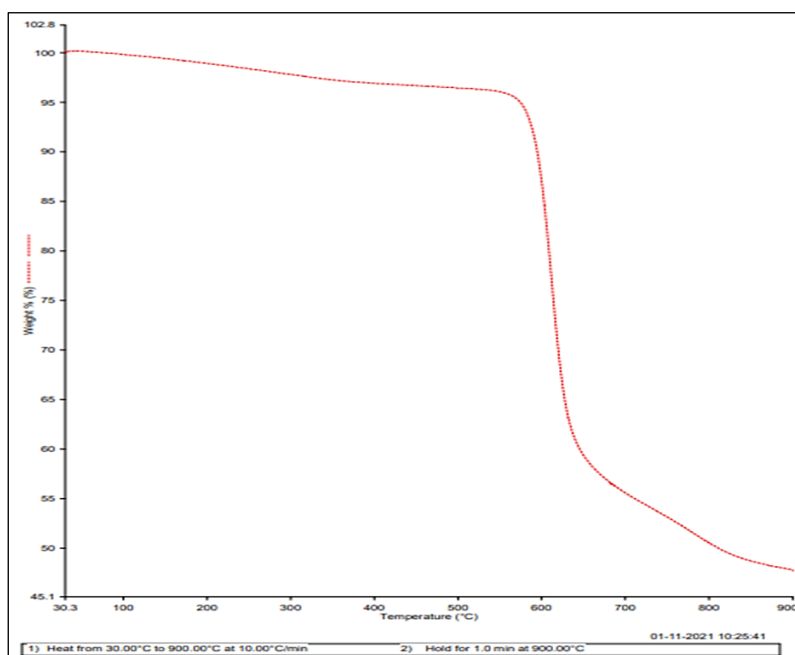


**Figure 10:** TGA Curve of Virgin PEEK, Indicating Weight Loss Pattern of PEEK under Influence of Heat

**Table 9:** A Comparison of Properties of Various Biomaterials

Properties	PLA	PGA	PLGA	Chitosan	This work
Tensile Strength	PLA is 39.9 MPa to 52.5 MPa (57-59)	PGA is 80-90 MPa. (60, 61)	PLGA is 40 - 60 MPa. (62-64)	Chitosan 20-50 MPa. (65-67)	51.52 MPa
Thermal Properties	Tg: ~55-60°C; low thermal resistance (58)	Tg: ~35-40°C; moderate thermal resistance. (61)	Varies with PLA:PGA ratio (40-55°C). (63)	Low thermal stability; degrades around 150°C (65-67)	Thermal stability up to 558°C

**X ray Diffraction of Pure PEEK**

The characteristics of the materials used in XRD patterns reflects the nature of the XRD pattern's Bragg's peaks Peak intensity reveals the atomic position inside a lattice structure and Peak width reveals crystalline nature and lattice strain. The

figure 11 shows PEEK XRD patterns, the three peaks around 2θ range between 17° to 25° can be observed to the {110}, {113} and {200} crystallographic planes of crystallized PEEK, respectively.

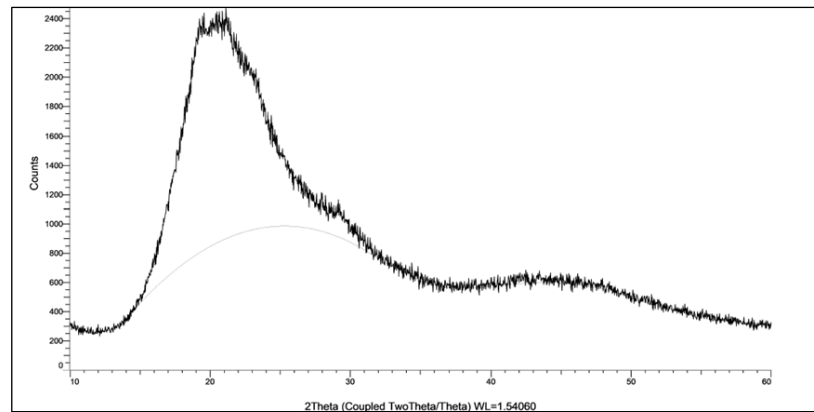


**Figure 11:** XRD Spectra of PEEK

Above  $40^\circ$  shows low intensity amorphous peaks, as a whole PEEK shows a semi crystalline nature of high-performance thermoplastic polymer often detected around  $2\theta = 18^\circ\text{--}23^\circ$  and  $2\theta = 28^\circ\text{--}30^\circ$ . The broad peak after  $40^\circ$  in the provided XRD spectrum suggests the dominance of amorphous regions, with limited crystalline domains. The unique feature of PEEK materials is their highly organized molecular structure, which results in sharp melting points. Semi-crystalline materials, like PEEK, rapidly soften with temperature is raised, in contrast to amorphous materials. Moreover, annealing or processing conditions can shift the degree of crystallinity and peak intensities.

### Scanning Electron Microscopy of 3D Printed Specimens

The samples were prepared for scanning electron microscopy (SEM) imaging by sputter coating with a thin layer of gold alloy. Imaging was performed

using the high vacuum/secondary electron imaging mode at an accelerating voltage of 20.0 kV and at magnifications of 200X, 2000 X, 5000 X, and 30,000 X. It has been observed that majority of the region under microscopic image is a smooth surface. However, it is also clear that some surface has irregular pile up, flaky surface with minor cracks of printed PEEK due to non-homogenous layer adhesion and improper fusion temperature condition during the 3D print. As per the surface morphology of figure 12, PEEK fabricated via FDM often exhibits rough surfaces and voids, consistent with the observed features. The image clearly shows pits on the PEEK surface. These pits are irregular and might result from thermal fluctuations during the 3D printing process or insufficient fusion between the deposited layers. Roughness and pits on the surface can be advantageous for biomedical implants, enhancing Osseo integration and cell proliferation.

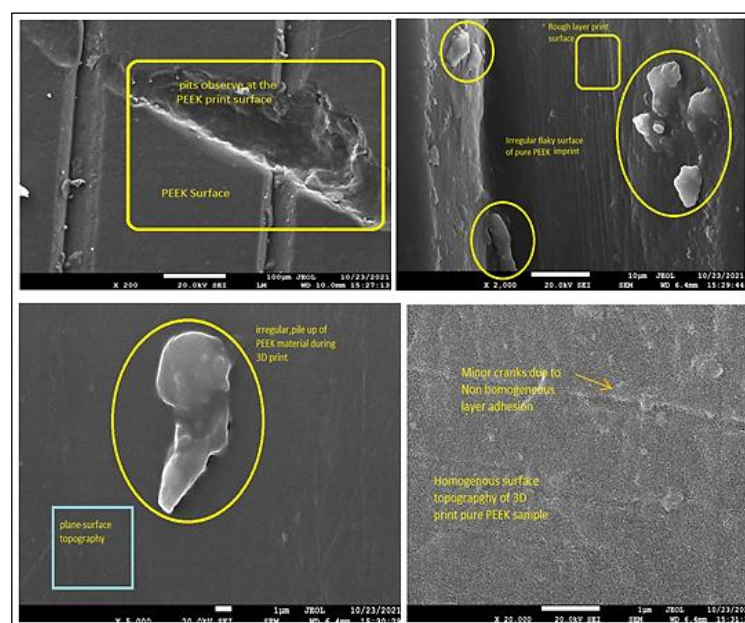


**Figure 12:** SEM Images of 3D Printed Specimens

### Cell Culture

L929 which is a mouse fibroblast cell line, were ordered from National Centre for Cell Science (NCCS, Pune) were grown in Dulbecco modified Eagle medium (DMEM) (GIBCO Laboratories) supplemented with 10% fetal bovine serum (FBS), 25 mM glucose, penicillin 100 IU/mL, and streptomycin 100 g/mL at 37°C in 95% air and 5% CO<sub>2</sub>.

### MTT Assay

The MTT [or 3-(4, 5-dimethyl-2-yl)-2, 5-diphenyl tetrazolium bromide] assay was done to assess sensitive and reliable indicators of the cellular

metabolic activity of the biomaterial on L929 cell line. Cells were sub cultured in 96-well plates and grown to 80% to 90% confluence. Subsequently, cells were exposed to various concentrations of biomaterial (0.6 to 3 µg/ml) and incubated for 24 hours. After that, PBS washing was given followed by treatment with MTT (5mg in 10ml) and incubated for 2-4 hours in a CO<sub>2</sub> incubator. At the end formazan crystal formed by mitochondrial reduction of MTT were solubilized in DMSO (100 µL/well) and the absorbance was read at 570 nm. The experiments were conducted in triplicates (n=3).

$$\text{Cell proliferation} = (\text{Sample OD} \div \text{control OD}) \times 100$$

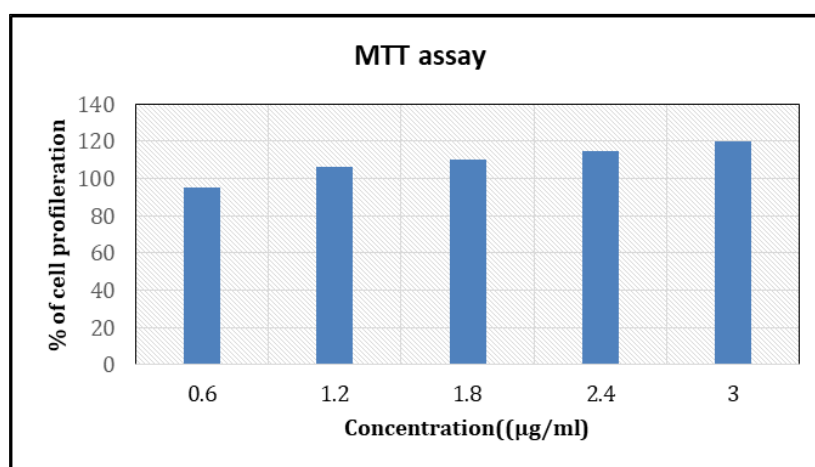


**Figure 13:** MTT Assay Plot Shows Concentration vs % Cell Proliferation

It is widely accepted that the initial interactions between the cells and implant surface are crucial to clinical success and improvement can lead to faster bone formation (68). As seen in the graph figures 13 PEEK exhibit cell proliferation activity, inversely proportional to concentration. Hence, selected biomaterial is having good viability and does not inhibit the growth. Also, the selected PEEK is biocompatible and could be used for a biomedical application.

### Conclusion

Biomaterials are designed to enhance or replace the functions of tissues or organs within the human body. An experimental study was conducted to know the potential capability of mechanical properties of PEEK to test the suitability for biomedical application.

- The finish produced by the FDM process meets clinical acceptability threshold for biomedical implants, with a surface roughness Ra value close to 0.2 micrometres.
- Maximum Tensile strength at peak load of

1988 N is observed to be 51.52 MPa conducted as per ASTM D638 standards. The Young Modulus found to be 1435.75 MPa. The infill pattern selected was along the direction of applied tensile load. The maximum compressive strength of 3D print was examined to be 279.91 MPa at a peak load of 87775 N, carried out in accordance with ASTM D695. This compressive strength value is caused by an infill pattern that runs circumferentially. ASTM D256 impact test shows maximum value of 30.78 KJ/m<sup>2</sup> at applied load by selecting infill pattern orientation perpendicular to the applied load.

- Based on thermal characteristics, Virgin PEEK began to degrade gradually approximately at 560°C. Around 550° C, the remarkable weight loss occurred due to the loss of decomposition products of PEEK. The TGA thermographs show that the best temperature settings for 3D printing are before 550° C.
- The XRD spectroscopy analysis of pure PEEK

indicated a well-defined molecular structure and distinct melting points, indicating its semi-crystalline nature.

- The irregular pile up, flaky surface, and tiny cracks of the print surface originate from non-homogeneous layer adhesion and inappropriate fusion temperature conditions during the 3D print.
- The findings in the cell culture study reveal that the PEEK biomaterial exhibits excellent biocompatibility, as evidenced by its ability to support cell proliferation without inhibiting growth, even at varying concentrations.

It can be concluded, that PEEK 3D print surface is suitable for various biomedical applications.

### Abbreviations

AM: Additive Manufacturing, PEEK: Polyetheretherketone, CAD: Computer Aided Design, SME: Society of Manufacture Engineers, STL: Standard Triangle Language, FDM: Fused Deposition Modelling Computed Tomography imaging, CT imaging: Computed Tomography imaging, PAEK: Polyaryletherketone, ASTM: American Society for Testing and Materials, MPa: Mega Pascal, TGA: Thermo Gravimetric Analysis, XRD :X-Ray Diffraction, SEM: Scanning Electron Microscope.

### Acknowledgment

This work was done without any support from any supporting agency, facility, or public agency.

### Author Contributions

Material preparation, Data collection, Testing and analysis, Manuscript preparation, subsequent revisions was done by Mr. Jasvir Singh. Study's conception and design, Statistical analysis was done by Dr. Vishal Francis. All the authors have read and approved the final manuscript.

### Conflicts of Interest

The authors declare that they have no conflicts of interest.

### Ethics Approval

Not applicable.

### Funding

It is certified that researchers did not receive any particular grant from funding agencies in the public, commercial, or not-revenue-driven sectors.

## References

1. Campbell I, Bourell D, Gibson I. Additive manufacturing: rapid prototyping comes of age. *Rapid Prototyping Journal*. 2012;18(4): 255 – 258.
2. Negi S, Dhiman S, Sharma R K. Basics and applications of rapid prototyping medical models. *Rapid Prototyping Journal*. 2014; 20(3):56 –267.
3. Campbell R I, Dickens P M. *Rapid Prototyping: A Global View. Solid Freeform Fabrication: An Advanced Manufacturing Approach. 5th Solid Freeform Fabrication Symposium Proceedings. Centre for Materials Science and Engineering Univ. of Texas, Austin. 1994; 110-117.*
4. Milovanovic J, Trajanovic M. Medical applications of Rapid Prototyping. *Facta Universitatis Series: Mechanical Engineering*. 2007;5(1):79 – 85.
5. Upcraft S, Fletcher R. The rapid prototyping Technologies. *Emerals Assembly Automation*. 2003;23(4):318–330.
6. Haleem A, Javaid M. Polyether ether ketone (PEEK) and its 3D printed implants applications in medical field: An overview. *Clinical epidemiology and global health*.2019;7(4):571-577.
7. Medical Additive Manufacturing/3D printing SME. *Medical Manufacturing Innovations; Annual Report*. 2018; 070520174.
8. Cui X, Boland T, Dlima D D, Lotz M K. Thermal inkjet printing in tissue engineering and regenerative medicine. *Recent Pat Drug Deliv Formula*. 2012;6(2):149–55,
9. Schubert C, Van Langeveld MC, Donoso LA. Innovations in 3D printing: a 3D overview from optics to organs. *Br J Ophthalmol*. 2014; 98(2):159–161.
10. Banks J. Adding value in additive manufacturing: researchers in the United Kingdom and Europe look to 3D printing for customization. *IEEE Pulse*. 2013; 4(6):22-26.
11. Mertz L. Dream it, design it, print it in 3-D: What can 3-D printing do for you. *IEEE Pulse*. 2013; 4(6):15-21.
12. Ibrahim A M S, Jose R R, Rabie A N, Gerstle T L, Lee B T, Lin S J. Three-dimensional printing in developing countries plastic and reconstructive surgery. *Glob Open J*. 2015; 3(7): e443.
13. Rankin T M, Glovinco N A, Cucher D J, Watts G, Hurwitz B, Armstrong DJ. Three-dimensional printing surgical instruments: are we there yet. *J Surg Res*. 2014;189(2):193-7.
14. Ursan I, Chiu L, Pierce A. Three-dimensional drug printing: a structured review. *J Am Pharm Assoc*. 2013;53(2):136–144.
15. Lee A Y, Jia A N, Chua C K. Two-way 4D printing: a review on the reversibility of 3D-printed shape memory materials; *Engineering*. 2017; 3(5): 663-674.
16. Perez B, Nykvist H, Brogger A F, Larsen M B, Falkeborg M F. Impact of macronutrients printability and 3D-printer parameters on 3D-food printing: a review. *Food Chem*. 2019; 287:249–257.
17. Chen Z, Li Z, Li J, Liu J, Liu C, Lao C, Fau Y, Liu C, Li Y, Wang P, He Y. 3D printing of ceramics: a review. *J Eur Ceram Soc*. 2019; 39(4): 661–687.
18. Blok L G, Longana M L, Yu H, Woods B K S. An investigation into 3D printing of fibre reinforced

- thermoplastic composites. *Addit Manufacturing*. 2018; 22:176–186.  
<https://doi.org/10.1016/j.addma.2018.04.039>
19. Zarek M, Mansour N, Shapira S, Cohn D. 4D printing of shape memory-based personalized endoluminal medical devices. *Rapid Commun*. 2017; 38:233–244.
  20. Pop M A, Croitoru C, Bedo T, Geaman V. Structural changes during 3D printing of bioderived and synthetic thermoplastic materials. *J Appl Polym Sci Symp*. 2019; 136:473–482.
  21. Lin Y H, Chuang T Y, Chiang W H, Chen W P, Wang K, Shie-M Y, Chen Y W. The synergistic effects of graphene-contained 3D-printed calcium silicate/poly- $\epsilon$ -caprolactone scaffolds promote FGFR-induced osteogenic/angiogenic differentiation of mesenchymal stem cells. *Mater Sci Eng C Mater Biol Appl*. 2019;104: 109887.
  22. Garreta E, Oria R, Tarantio C, Roca M P, Prado P, Aviles F F, Campistol J M, Samitier J, Montserrat N. Tissue engineering by decellularization and 3D bioprinting. *Mater Today*. 2017; 20:166–178.
  23. Kumar R, Kumar S. Trending applications of 3D printing: a study. *Asian Journal of Engineering and Applied Technology*. 2020; 9(1):1-12.
  24. Milewski J O. Trends in AM, government, industry, research, business, additive manufacturing of metals. *Springer Ser Mater Sci*. 2017; 258:255–292.
  25. Wu Y H, Chiu Y C, Lin Y H, et al. 3D-printed bioactive calcium silicate/poly- $\epsilon$ -Caprolactone bio scaffolds modified with biomimetic extracellular matrices for bone regeneration. *Int J Mol Sci*. 2019;20:942.
  26. Huang KH, Chen YW, Wang CY, Ho C C, Shie M Y, Chen Y W. Enhanced capability of BMP-2-loaded mesoporous calcium silicate scaffolds to induce odontogenic differentiation of human dental pulp cells. *Endod*. 2018; 44:1677–1685.
  27. Basgul C, Yu T, MacDonald DW, Siskey R, Marcolongo M, Kurtz SM. Structure property relationships for 3D-printed PEEK intervertebral lumbar cages produced using fused filament fabrication. *J Mater Res*. 2018; 33(14):2040–2051.
  28. Rae P J, Brown E N, Orlor E B. The mechanical properties of poly (ether-ether-ketone) (PEEK) with emphasis on the large compressive strain response. *Polymer (Guildf)*. 2007; 48:598–615.
  29. Rahmitasari F, Ishida Y, Kurahashi K, Matsuda T, Watanabe M, Ichikawa T. PEEK with reinforced materials and modifications for dental implant applications. *Dent J*. 2017;5(4):35.
  30. Choudhury A, Chakraborty D, Reddy B. Extruder path generation for Curved Layer Fused Deposition Modeling. *Computer-aided design Journal*. 2007; 40:235- 243.
  31. Anitha R, Arunachalam S, Radhakrishnan P. Critical parameters influencing the quality of prototypes in fused deposition modeling. *Journal of Materials Processing Technology*. 2001; 113(1-3): 385-388.
  32. Panayotov I V, Orti V, Cuisinier F, Yachouh J. Polyetheretherketone (PEEK) for medical applications. *J Mater Sci: Mater Med*. 2016;27:118.
  33. Haleem A, Javaid M. Polyether ether ketone (PEEK) and its 3D printed implants applications in medical field: An overview; *Clinical Epidemiology and Global Health*. 2019; 7(4):571-577.
  34. Zhao F, Li D, Jin Z. Preliminary investigation of Poly-Ether- Ether- Ketone based on Fused deposition modeling for medical applications. *Materials*. 2018;11(2):288.
  35. Chhabra, M. and Singh, R. Rapid casting solutions a review. *Rapid Prototyping Journal*. 2011;17(5),328-350.
  36. Masood S H. Intelligent rapid prototyping with fused deposition modelling. *Rapid Prototyping Journal*. 1996; 2(1):24-32.
  37. Singh R, Singh, S. Development of nylon based FDM filament for industrial applications. *Journal of Institution of Engineers (Series-C, Springer)*. 2014;92(2):103- 108.
  38. Ramazani H, Kami A. Metal FDM, a new extrusion-based additive manufacturing technology for manufacturing of metallic parts: a review. *springer link- Progress in Additive Manufacturing*. 2022;7(8): 609-626.
  39. Hoque M E, Chuan Y L, Pashby I. Extrusion based rapid prototyping technique: An advanced platform for tissue engineering scaffold fabrication. *Biopolymers*. Wiley online library. 2011; 97(2):83-93.
  40. Singh R, Singh S, Mankotia K. Development of ABS based wire as feedstock filament of FDM for industrial applications. *Rapid Prototyping Journal*. 2016; 22(2): 300-310.
  41. Algarni M, Ghazali S. Comparative Study of the Sensitivity of PLA, ABS, PEEK, and PETG's Mechanical Properties to FDM Printing Process Parameters. *Crystals*. 2021; 11(8): 995.
  42. Abbas K, Hedwig L, Balc N, Bremen S. Advanced FFF of PEEK: Infill Strategies and Material Characteristics for Rapid Tooling. *Polymers*. 2023; 15(21):4293
  43. Dezaki M L, Ariffin M K A M. The Effects of Combined Infill Patterns on Mechanical Properties in FDM Process. *Polymers*. 2020; 12(12): 2792.
  44. Rendas P, Figueiredo L, Claudio R, Vidal C, Soares B. Investigating the effects of printing temperatures and deposition on the compressive properties and density of 3D printed Polyetheretherketone. *Progress in Additive Manufacturing*. 2023; 9(6):1883-1899.
  45. Mutyala R S, Park K, Gunay E E, Kim G, Lau S, Jackman J, Kremer E O. Effect of FFF process parameters on mechanical strength of CFR-PEEK outputs. *International Journal on Interactive Design and Manufacturing*. 2022; 16:1385–1396.
  46. Mushin S A, Hatton P V, Jhonson A, Sereno N, Wood D J. Determination of Polyetheretherketone (PEEK) mechanical properties as a denture material. 2019;31(3); 382-391.
  47. Mrowka M, Machochek T, Jureczko O, Jozsko k, Gzik M, Wolenski W, Wilk K. Mechanical, Chemical, and Processing Properties of Specimens Manufactured from Poly-Ether-Ether-Ketone (PEEK) Using 3D Printing. *Materials*. 2021;14(11): 2717.
  48. Yang C, Tian X, Dichen LI, Cao Yi, Feng Z, Shi C. Influence of thermal processing conditions in 3D printing on the crystallinity and mechanical properties of PEEK material. *Journal of Materials Processing Technology*, 2017;248:(1-7).
  49. Elawadly T, Radi I A, Khadem A E, Osman R B. Prognosis of dental implants in patients with low bone density: A systematic review and meta-analysis. *Journal of Oral Implantology*. 2018;

- 43:456-461.
50. Heimer S, Schmidlin P R, Roos M, Stawarczyk B. Surface properties of polyetheretherketone after different laboratory and chairside polishing protocols. *J Prosthet Dent.* 2017;117: 419-425.
  51. Alp G, Johnston W M, Yilmaz B. Optical properties and surface roughness of prepolymerized poly (methyl methacrylate) denture base materials; *J Prosthet Dent.* 2019; 121:347-52.
  52. Francis V, Jain P K. Investigation on the effect of surface modification of 3D printed parts by nano clay and dimethyl ketone. *Materials and Manufacturing Processes.* 2017;33(10): 1080-1092.
  53. Barfeie A, Wilson J, Rees J. Implant surface characteristics and their effect on osseointegration. *Nature, British dental journal.* 2015;289(5):292-293.
  54. Alla R K, Ginjupalli K, Upadhya N, Shammam M, Ravi R K, Sekhar R. Surface Roughness of Implants: A Review. *Trends Biomater. Artif. Organs.* 2011; 25(3): 112-118.
  55. Burgers R, Gerlach T, Hahnel S, Schwarz F, Handel G, Gosau M. In vivo and in vitro biofilm formation on two different titanium implant surfaces. *Clin Oral Implants Res.* 2010; 21(2):156-64.
  56. Batak B, Cakmak G, Johnston W M, Yilmaz B. Surface roughness of high-performance polymers used for fixed implant-supported prostheses. *The Journal of prosthetic dentistry,* 2021;126(2):254.
  57. Kholil A, Asyaefudin E, Pinto N, Syaripuddin S. Compression Strength Characteristics of ABS and PLA Materials Affected by Layer Thickness on FDM. *Journal of Physics: Conference Series.* 2022; 2377 012008.
  58. Dou H, Ye W, Zhang D, Cheng Y, Tian Y. Compression Performance with Different Build Orientation of Fused Filament Fabrication Polylactic Acid, Acrylonitrile Butadiene Styrene, and Polyether Ether Ketone. *Journal of Materials Engineering and Performance.* 2022;31(3):1925-1933.
  59. Musa L, Kumar N K, Rahim S Z A, Rasidi M S M, Rennie A E W, Rahman R, Kanani A Y, Azmi A A. A review on the potential of polylactic acid based thermoplastic elastomer as filament material for fused deposition modelling. *Journal of Materials Research and Technology.* 2022;20(9-10): 2841-2858.
  60. Ahlfeld T, Lode A, Placht A M, Fecht T, Wolfram T, Grom S, Hoess A, Vater C, Brauer C, Heinemann S, Lauer G, Reinauer F, Gelinsky M. A comparative analysis of 3D printed scaffolds consisting of poly(lactic-co-glycolic) acid and different bioactive mineral fillers: aspects of degradation and cytocompatibility. *Biomater Sci.* 2023; 11: 5590-5604. <https://doi.org/10.1039/D2BM02071H>
  61. Aihemaiti P, Jia R, Aiyiti W. Study on 3D printing process of continuous polyglycolic acid fiber-reinforced polylactic acid degradable composites. *Int J Bioprint.* 2023; 9(4): 734.
  62. Feuerbach T, Mendoza S C, Thommes M. Development of filaments for fused deposition modeling 3D printing with medical grade poly(lactic-co-glycolic acid) copolymer. 2019;24(4); 487-493.
  63. Dastidar A G, Clarke S A, Larraneta A, Buchanan F, Manda K. In Vitro Degradation of 3D-Printed Poly (L-lactide-Co-Glycolic Acid) Scaffolds for Tissue Engineering Applications. *Polymers.* 2023; 15(18): 3714.
  64. Zhao D, Zhu T, Li, J, Cui L, Zhang Z, Ding J. Poly (lactic-co-glycolic acid)-based composite bone-substitute materials. *Bioactive Materials.* 2021; 6(2):346-360.
  65. Abinaya B, Prasith T P, Ashwin B, Chandran S V, Selvamurugan N. Chitosan in Surface Modification for Bone Tissue Engineering Applications. *Biotechnology journal.* 2019;14(12):1900171.
  66. Mania S, Banach A, Tylingo R. Review of current research on chitosan as a raw material in three-dimensional printing technology in biomedical applications. *Progress on Chemistry and Application of Chitin and Its Derivatives.* 2020; 37-50.
  67. Singh S, Singh G, Prakash C, Ramakrishna S, Lamberti L, Pruncu L. 3D printed biodegradable composites: An insight into mechanical properties of PLA/chitosan scaffold. *Polymer Testing.* 2020; 89:106722.
  68. Tooth J M. Chapter 8 - Biocompatibility of PEEK Polymers. *PEEK Biomaterials Handbook (Second Edition)- Plastics Design Library.* 2019; 2nd Edition:107-119.